Mineralogical Magazine, October 1998, Vol. 62(5), pp. 585–598

Phase transitions in silicate perovskites from first principles

MICHELE C. WARREN[1], GRAEME J. ACKLAND, BIJAYA B. KARKI AND STEWART J. CLARK

Department of Physics and Astronomy, The University of Edinburgh, James Clerk Maxwell Building, The King's Buildings, Mayfield Road, Edinburgh EH9 3JZ, UK

ABSTRACT

The equilibrium structures of cubic, tetragonal and orthorhombic phases of magnesium silicate perovskite are found from first principles electronic structure calculations. Zone centre and zone boundary phonons of each phase are also calculated from *ab initio* forces from finite displacments, and phase transitions between the phases are analysed in terms of phonon instabilities, and coupling between modes. Both the cubic and tetragonal phases have strongly unstable modes dominated by rotation of the SiO_6 octahedra, which freeze in to ultimately form the orthorhombic phase. First priniciples molecular dynamics simulations at finite temperatures are used to further investigate the stability of the intermediate tetragonal phase and the coupling between participating phonon modes. The implications for a transition temperature between orthorhombic and tetragonal phases are discussed.

KEYWORDS: perovskite, phase transition, phonon, silicate.

Introduction

MAGNESIUM silicate perovskite makes up most of the material in the Earth's lower mantle, and its properties and phase transitions have important implications for the macroscopic behaviour of the mantle (Catlow and Price, 1990; Navrotsky and Weidner, 1989). Despite this, studies using a variety of theoretical and experimental techniques (Navrotsky and Weidner, 1989; Hemley and Cohen, 1992; Hemley *et al.*, 1987; Mao *et al.*, 1991; Ross and Hazen, 1990) have yet to completely determine the properties of $MgSiO_3$ or understand its structural and thermodynamic behaviour. However, by comparison with other perovskites, especially $SrTiO_3$, an orthorhombic–tetragonal–cubic series of transitions may be envisaged. This has had some support from observations of twinning in the orthorhombic phase, after quenching from high temperature (Wang *et al.*, 1992). We describe here investigations into the possibility of such transitions under mantle conditions, using first principles electronic structure simulations.

We consider three phases related by successive symmetry-breaking transitions: the hypothetical cubic phase (*Pm3m*) at high *T*, the observed orthorhombic (*Pbnm*) phase (low *T*) and an intermediate tetragonal phase (*I4/mcm*). Transitions between these phases involve only small displacements of the atoms, and do not involve changes in coordination. They are thus likely to proceed via soft-mode mechanisms (Hemley and Cohen, 1992), in which a vibrational mode of a high-symmetry phase becomes unstable, precipitating a permanent distortion. The zone-centre phonons of several other perovskites found from first principles have already been shown to correspond to observed phase transitions (Cohen and Krakauer, 1990; Postnikov *et al.*, 1994; King-Smith and Vanderbilt, 1994). However, in $MgSiO_3$ the orthorhombic unit cell is related to the cubic by two 'cell-doubling' procedures (Lines and Glass, 1977), so any phonons involved in the transition between these phases must lie at either the zone centre or the zone boundary of the cubic phase. A simulation of more than one cubic unit cell is required to calculate the relevant phonons within

[1] Present address: Department of Earth Sciences, University of Cambridge, Downing Street, Cambridge CB2 3EQ UK.

the constraints of periodic boundary conditions. Recently a similar phase transition has been proposed in $CaSiO_3$ (Stixrude *et al.*, 1996).

The corner-sharing octahedral units comprised of oxygen ions which form all three phases are shown in Fig. 1, and each contains a silicon (B) ion in the centre. In the voids between the octahedra there are 12-fold coordinated magnesium (A) ions. In the cubic phase (*Pm3m*), the octahedra are aligned along the cubic axes, but in the orthorhombic structure they are rotated around the silicon ions, and the magnesium ions are displaced, giving space group *Pbnm*. This is the form of $MgSiO_3$ assumed to be dominant in the lower mantle. The tetrahedral structure is a hypothetical intermediate structure, and will be described further below.

The CASTEP (Payne *et al.*, 1992) and CETEP (Clarke *et al.*, 1992) total energy codes were used, employing norm-conserving, nonlocal, Kleinman-Bylander pseudopotentials (Kleinman and Bylander, 1982; Kerker, 1980). Details are given elsewhere (Warren and Ackland, 1996). A fully transferable pseudopotential for magnesium has been found hard to generate, due to the lack of *p* electrons in the ground state, and recently we repeated some of our calculations with a more satisfactory pseudopotential, which treats equally all angular momentum components of the wavefunctions (Karki *et al.*, 1997). This lead to an equilibrium volume much closer to the experimental value and has been used in all subsequent work. This potential is used in the latter section of this paper, with an energy cutoff of 700 eV and generalised gradients corrections for electron exchange and correlation. Phonon frequencies were affected by less than 10% by the change of potential, and were consistent with the change in equilibrium volume.

The probable mechanism of any transitions between the three phases is deduced from our investigations (Warren and Ackland, 1996) which

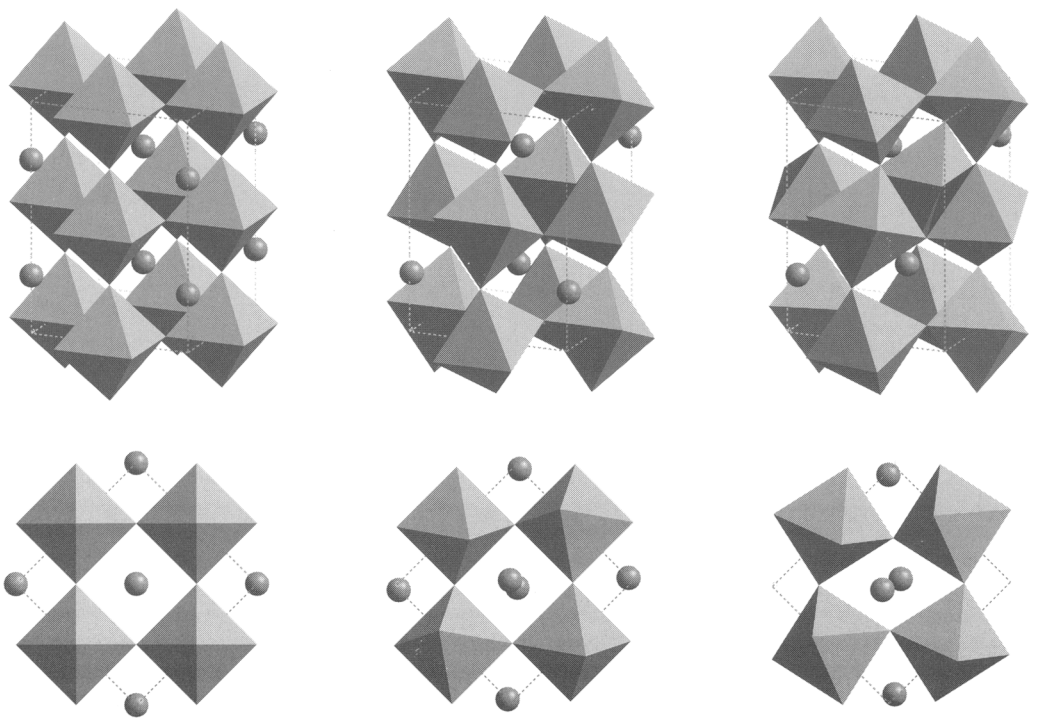

FIG. 1. Cubic, tetragonal and orthorhombic structures of $MgSiO_3$ perovskite. Twenty atoms of each structure are drawn (four unit cells of the cubic phase; one of the orthorhombic).

are summarised here. However, since only the zero temperature state is simulated, transition temperatures are not obtained, nor is it possible to determine if the tetragonal phase does in fact form a distinct intermediate phase over any temperature range. Molecular dynamics simulations at finite temperatures may be able to solve some of these problems, and initial results and methodology are presented here.

Traditionally, molecular dynamics simulations have used an empirical potential to calculate the forces between atoms in any given configuration so that the equations of motion may be integrated forwards in time. Time-averaged system properties may then be measured and analysed. However, in 1985 the Hellmann-Feynman forces obtained from plane-wave pseudopotential calculations were first used instead (Car and Parrinello, 1985), and *ab initio* MD has become an established technique (Oguchi and Sasaki, 1991; Clark and Ackland, 1997). The large computational requirements of such simulations still mean that only modest numbers of atoms may be considered, rather than the more realistic samples which may be simulated using empirical potentials. However, with increasing computational power such first-principles simulations are becoming more routine. Alternative strategies include using *ab initio* calculations to parameterise model potentials, which may be used to perform much larger simulations (Rabe and Waghmare, 1996), but in that case the appropriate variables must be deduced without loss of potentially important secondary effects. Detailed first principles calculations therefore also have a role to play in identifying suitable variables.

Equilibrium structures from first principles

The plane-wave basis set used to expand the electronic wavefunctions is independent of the positions of the ions, so the forces on the ions in any given configuration may be calculated to arbitrary accuracy using the Hellmann-Feynman theorem (Payne *et al.*, 1992). The internal stress on the unit cell may also be calculated from first principles. However, the plane wave basis set is determined by the reciprocal lattice, so there is an energy change associated with a change of unit cell and thus a spurious stress. A Pulay correction has been implemented (Francis and Payne, 1990; Hsueh *et al.*, 1996) to correct for this effect.

The complete structure of each phase may thus be relaxed to equilibrium under first principles forces and stresses, using a combination of conjugate gradients and quenched molecular dynamics algorithms (Warren and Ackland, 1996). The initial symmetry of each phase may be preserved by symmetrising the forces and stresses. However, this approach means that lower-symmetry phases will need to be explicitly considered since the symmetry will not be broken spontaneously. Suitable distortions may be determined by finding either low energy, or unstable, phonon modes of the structure. Reconstructive phase transitions involving more drastic changes of bonding topology will not be indicated by this process although they may still be studied if the end-points are known.

The structural parameters obtained for $MgSiO_3$ were presented and discussed elsewhere (Warren and Ackland, 1996; Karki *et al.*, 1997); the orthorhombic phase was found to be 8% denser than the cubic. The structural parameters still followed the reported trend of an increase in distortion under compression (Hemley *et al.*, 1987; Wentzcovitch *et al.*, 1993; Matsui, 1988), although the Si–O bondlength was only 1% smaller than that observed.

Phonons

To find a set of zone-centre and zone-boundary phonons, the dynamical matrix of effective spring constants Φ is required for four formula units of each phase. In the harmonic approximation these may be defined according to the force acting on the κth atom in the lth supercell when all atoms are displaced by $u_\beta(^{l'}_{\kappa'})$:

$$F_\alpha(^{l}_{\kappa}) = \sum_{l'} \sum_{\kappa'} \sum_{\beta} \Phi_{\alpha\beta}(^{l\,l'}_{\kappa\kappa'}) u_\beta(^{l'}_{\kappa'}) \qquad (1)$$

The set of spring constants may thus be obtained by finding the Hellmann-Feynman forces when each atom is displaced in turn by a small amount, using a scheme we have presented elsewhere (Warren and Ackland, 1996; Hsueh *et al.*, 1996). Not all ionic coordinates need to be perturbed since the space-group symmetry may be used to complete the matrix from a minimal set of simulations. This scheme gives reliable information about phonons at wavevectors which are reciprocal lattice vectors of the simulation cell, due to the only use of periodic boundary conditions over a distance smaller than the range of the interatomic interactions.

Phonons at the zone centre have strictly $\mathbf{k} = 0$, and macroscopic dipoles are not possible in a scheme with periodic boundary conditions. The

calculated phonons are thus TO and TA modes, i.e. LO/TO splitting due to long-range dipole interactions is not accessible. However, LO/TO splitting will stiffen the LO frequency but not affect the TO modes. The most unstable modes are thus calculated accurately in this scheme, and are the modes of interest for possible soft-mode transitions. The twenty-atom cell shown in Fig. 1 allows direct calculation of phonons at the Γ, *X*, *M* and *R* points of the cubic Brillouin Zone.

Cubic phase

The cubic phase has an unstable mode at the zone centre, having an imaginary frequency, which is dominated by motion of the magnesium (A) ions against the rest of the crystal. This is in contrast to many other perovskites, in which it is the B atoms which 'rattle' inside the oxygen cage (King-Smith and Vanderbilt, 1994; Lines and Glass, 1977). Since there is no evidence of strong covalent Si–O bonds in $MgSiO_3$, this motion is probably due to the relative sizes of the oxygen, silicon and magnesium ions (Hemley *et al.*, 1987; King-Smith and Vanderbilt, 1994): magnesium is one of the smallest cations. The frequencies obtained are shown in Fig. 2.

The eigenvectors of all the phonons were also obtained from the dynamical matrix. The most unstable modes were found at *R* and *M* (around 12*i* THz), consisting of rotations of near-rigid octahedra around the silicon atoms. At *M*, the mode involves rotation about *z*, and has M_2 symmetry; rotations at *R* are around all three axes and denoted R_{25}. These modes have been previously predicted to be the only zone-boundary rigid unit modes in cubic perovskites (Giddy *et al.*, 1993) and were also found in other theoretical studies (Hemley *et al.*, 1987; Stixrude and Cohen, 1993; Bukowinski and Wolf, 1988).

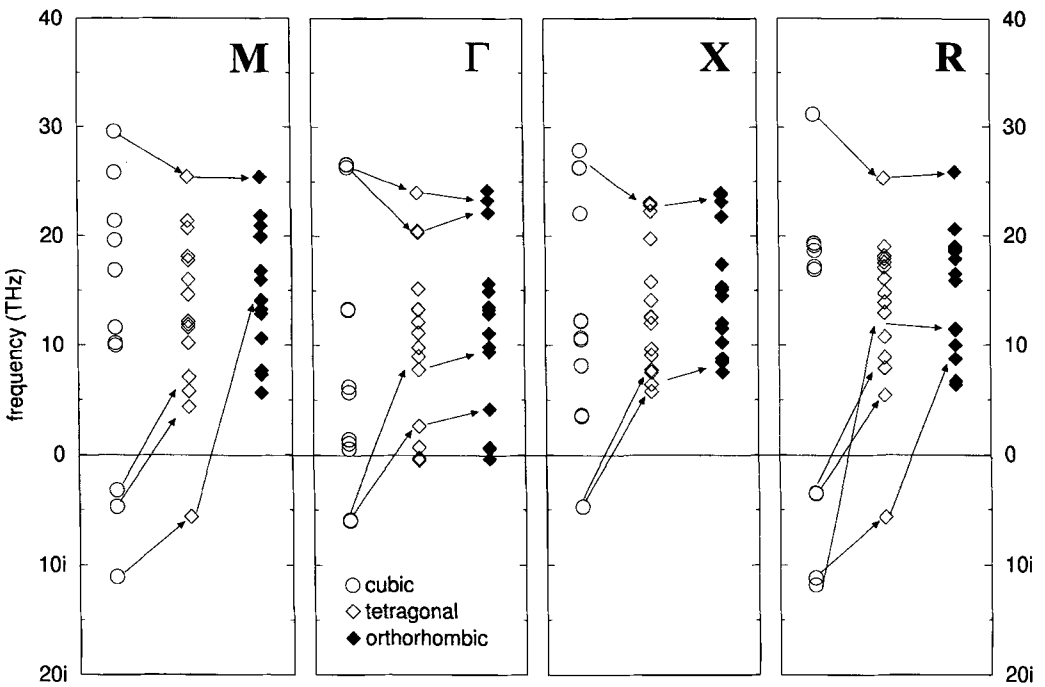

FIG. 2. Cubic, tetragonal and orthorhombic phonons at each part of the Brillouin Zone of the corresponding cubic phonon. There are unstable phonons at all parts of the Brillouin Zone in the cubic phase, but all the phonons in the orthorhombic phase are stable. The horizontal axes trace the progression from cubic to orthorhombic; arrows link phonons with similar eigenvectors as the structure becomes more distorted. Loss of degeneracy is due to the choice of supercell.

Larger cells are more unstable with respect to the soft magnesium mode, which is consistent with a picture in which the Mg ions 'rattle' inside the voids in the structure. In contrast, the M_2 unstable mode was found to become more unstable under pressure. This coupling between the unit cell and a mode involving octahedral rotation is compatible with the rigid unit mode (RUM) theory (Giddy *et al.*, 1993) which approximates the SiO_6 octahedra as rigid entities. However, detailed studies of the energies, forces and stresses involved in a RUM in $MgSiO_3$ suggested that although the model has some qualitative success in describing the behaviour of the structure, the phonon extreme which preserves the cell volume has a slightly lower energy (Warren and Ackland, 1996).

Intermediate structures

Introducing some amplitude of either the R_{25} or M_2 unstable modes into the cubic phase creates a tetragonal structure, with unique axis determined by the axis of octahedral rotation. If at some amplitude of each mode, the structure stabilises to a local equilibrium, a new metastable phase is generated. This phase will have lower energy than the original structure. However, there may still be some unstable phonons, which correspond to unstable modes of the cubic phase which have not been frozen in. First principles simulation techniques allow such possibilities to be investigated without regard to whether proposed phases are sufficiently stable to be observed experimentally. Since phonon modes strictly imply ionic motion at constant volume, the lattice parameters of the cubic phase were initially retained when generating trial structures.

When the cubic R_{25} mode is frozen into the cubic supercell, a twenty atom body-centred cell (space group *I4/mcm*) is generated, which reflects the geometry of the orthorhombic phase. The cubic R_{25} mode is triply degenerate; rotation was chosen to follow that observed in the orthorhombic phase. Coupling to motion of the Mg ions along x was found, so this coordinate was also allowed to relax, inducing displacements closely following the eigenvector of another unstable mode of the cubic phase at R. The phase formed in this way may thus be described by two ionic structural parameters, or, alternatively, by introducing non-zero amplitudes of two cubic phonons. There is a further slight deviation from the exact symmetry of the R_{25} mode such that there are two independent oxygen displacements, which should strictly be considered as a third active mode, but in practice this has only a very small amplitude.

This structure has lower energy than the corresponding phase formed by freezing in the M_2 phase. This structure was thus chosen as a possible intermediate tetragonal phase between cubic and orthorhombic. We therefore consider the possibility that it might form a distinct thermodynamic phase.

The sixty phonons commensurate with this cell were found. These are the Γ and X modes of this phase, but the eigenvectors will be linear combinations of the Γ, X, M and R phonons of the cubic phase. They were thus compared to those in the cubic phase, by taking scalar products between eigenvectors of the two phases, so that each phonon of the tetragonal phase may be identified with its closest match in the cubic structure. In what follows phonons of all phases are denoted by the location in the cubic Brillouin Zone of the most similar cubic mode. The tetragonal and orthorhombic phonons are plotted against this part of the cubic Brillouin Zone in Fig. 2. This procedure was designed to enable comparisons and determinations of the effects of phase transitions on the vibrational properties.

Only two unstable modes were found in this structure: the R and M modes corresponding to rotation about the z axis, with the latter slightly more unstable. The eigenvector of the M mode is strongly related to that of the original cubic M_2 mode, although it is much less unstable. All other modes which were unstable in the cubic structure were stabilised on transformation to this tetragonal phase.

Phonons of orthorhombic phase

As expected, there were no unstable modes in the orthorhombic phase. Only the Γ phonons of the orthorhombic Brillouin Zone can be found, since only one unit cell is simulated, but again this corresponds to the Γ, X, M and R points of the cubic phase, due to the quadrupling of the unit cell. Like those of the tetragonal phase, these phonons were also matched with their closest cubic modes and are plotted in Fig. 2 as solid diamonds. The octahedral rotation modes described in the cubic and tetragonal phases were still clearly identifiable, and were further stabilised in frequency. The deviation from zero of the acoustic modes at Γ indicates the

inaccuracies in the phonon calculation due to anharmonicity and noise (Ackland *et al.*, 1997).

Roles of individual phonons

The tetragonal phase described above was formed by freezing a permanent amplitude of two phonons into the cubic phase. Likewise, the positions $\{\mathbf{R}_\kappa\}$ of the ions in the stable orthorhombic phase may also be described in terms of introducing a combination of phonons into the cubic phase; this is merely a change of variables. Pure phonon modes involve only displacements at constant volume, so only the fractional atomic positions in the orthorhombic cell were used (i.e. as if it had the same cell parameters as the cubic cell) and a small change in cell parameters could in principle be considered separately. The mass-reduced displacement from the cubic configuration, $\mathbf{d}_\kappa$, is found for each atom in the stable orthorhombic structure:

$$\mathbf{d}_\kappa = \sqrt{m_\kappa}[\mathbf{R}_\kappa(\text{orth}) - \mathbf{R}_\kappa(\text{cubic})] \quad (2)$$

Phonon coefficients c_j are then defined such that:

$$\mathbf{d}_\kappa = \sum_j c_j \mathbf{p}^j_\kappa \quad (3)$$

where $\mathbf{p}$ are the mass-reduced eigenvectors of the cubic crystal, deduced previously. The orthonormality of the eigenvectors $\mathbf{p}$ allows $\{c_j\}$ to easily be found from scalar products of $\mathbf{d}$ and $\{\mathbf{p}^j\}$. For the orthorhombic cell these coefficients are denoted c_0, and are shown in Table 1. Since Γ, X, M and R cubic phonon eigenvectors span the complete set of all possible ionic distortions in the twenty atom cell, all distortions not involving strain may be expressed in this way, although a harmonic eigenvector $\mathbf{p}^j$ will not necessarily describe the individual mode at large displacement.

Only four of the fifteen unstable modes and two of the 42 stable phonons of the cubic phase have significant non-zero coefficients. Phonons consisting predominantly of magnesium displacement contribute much more weakly than those involving octahedral rotations, and were found to be strongly coupled to the rotational modes. We assume, therefore, that the two rotational modes dominate the transitions. The energy has been parameterised in terms of the amplitudes of these modes as described elsewhere (Warren and Ackland, 1996).

The tetragonal phase proposed above may only contain non-zero amplitudes of phonons at Γ and R of the cubic phase, and the two non-zero c_0 at R are exactly those used to form this structure. The other four modes (at X and M) can therefore be assumed to freeze in from the tetragonal intermediate to form the orthorhombic phase, providing a natural pathway for a cubic–tetragonal–orthorhombic series of transitions; the rotational M_2 mode, which is one of these four, was found to still be unstable in the tetragonal phase. The final degree of freedom required to account for the seven positional parameters in the orthorhombic $MgSiO_3$ is that due to the two independent oxygen displacements in the tetragonal phase. The unstable modes of the higher-symmetry structures are therefore sufficient to account for the observed phase.

TABLE 1. Calculation of the coefficients of cubic phonons frozen into the orthorhombic distorted phase. Phonons are labelled by the point of the cubic Brillouin Zone at which they occur, and their rank out of all sixty phonons. where two ranks are indicated, phonons form degenerate pairs, but the amplitude is for the active combination

	Rank according to frequency	Frequency (THz)	c_0 ($\sqrt{\text{a.m.u.}}$ Å)	Description
R	(59–60)	11.8i	6.48	Octahedral rotation about xy
M	(57)	11.1i	4.35	Octahedral rotation about z
X	(50+51)	4.73i	3.24	Mostly Mg displacement
R	(47–48)	3.48i	0.841	Mostly Mg displacement
X	(30+31)	10.5	0.780	Mg and O1 displacement
M	(13)	19.6	0.210	Octahedral squash

Molecular dynamics simulations

In order to follow the dynamics of the $MgSiO_3$ perovskite system at finite temperatures, the same supercell configuration as before was used, containing four formula units. Since this cell has the appropriate geometry to contain the orthorhombic, tetragonal and cubic phases it should in principle be possible to detect any transitions between these phases.

The ions were initially assigned their positions in the tetragonal phase, with the cell vectors of the cubic phase. Since the maximum phonon frequencies are around 30 THz, i.e. minimum period than 33 fs, a timestep of 1.0 fs was used, and should be sufficient to accurately follow all ionic motion. All ions were initially given a random velocity according to a prescribed temperature, and the equations of motion integrated forwards in time with a Verlet algorithm. The random initial velocities assigned to the ions are chosen such that the centre of mass is stationary, but a small amount of motion does develop due to the use of a finite timestep. Such drifting was corrected by subtracting the displacement of the centre of mass before further analysis. The lattice vectors were not changed in response to the stress during the simulations as this would have required impracticable amounts of computer time.

After an initial period of equilibration, the temperature may be measured from the time-averaged kinetic energy. If the atoms start from their equilibrium positions, equipartition would be expected but any phase transitions during the simulation will of course release additional energy. It is expected that the tetragonal–cubic phase transition would require a temperature above the melting point (Warren and Ackland, 1996) (T_m is around 1800 K at 0 GPa), so instead we are interested in the orthorhombic–tetragonal phase transition, with some transition temperature T_c.

The CETEP code was used on the T3D parallel supercomputer at the Edinburgh Parallel Computing Centre. These simulations require extremely large amounts of CPU time, so it was not possible to perform as many iterations as might be desired at each temperature to produce highly accurate statistics. However, the initial results presented here should be sufficient to detect the transition into the orthorhombic state, and illustrate the methodology which will be continued in further calculations.

Following transitions using normal modes

Any configuration may be described in terms of freezing selected phonons into cubic phase. All modes are referred to by their location in the cubic Brillouin Zone and rank according to frequency (from §1 to §60 and as given in Table 1). According to this scheme, one combination of each of the degenerate pairs §47/48 (Mg displacement) and §59/60 (R_{25} octahedral rotation) form the tetragonal phase. To then form the orthorhombic phase requires contributions from §13, §57 (M_2 rotation) and one combination each of the degenerate pairs §30/31 and §50/51, all at X or M in the cubic phase (see Table 1).

The state of the system during a simulation is described in terms of the average coefficients $\{\langle c_j(t)\rangle_t\}$ of the cubic normal modes (rather than the positions of the ions $(\mathbf{R}_{l,\kappa}(t)\}$) by projecting the ionic displacement from the cubic phase at time onto each cubic phonon eigenvector in turn, in the same way as in the analysis of the constituent modes of the orthorhombic structure. A total distortion $|\mathbf{d}(t)|^2$ may also be defined, using (3),

$$|\mathbf{d}(t)|^2 = \sum_j c_j^2(t) = \sum m_\kappa[\mathbf{R}_\kappa(t) - \mathbf{R}_\kappa(\text{cubic})]^2 \tag{4}$$

which when time-averaged indicates the average deviation from the cubic structure. The term 'coefficient' is used in preference to 'amplitude' since it is the time-averaged displacement which is most relevant, rather than the amplitude of oscillations about it.

If a single set of phonons corresponded to perfectly harmonic normal modes of all three phases, then pure harmonic oscillation in each of these coefficients would be observed, possibly around some non-zero value. However, some mode mixing and degeneracy breaking occurs, in addition to anharmonicity. The coefficients $c_j(t)$ of cubic phonons will thus vary non-sinusoidally for any modes j which are far from normal modes of the orthorhombic phase. However, most modes are close enough to lead to useful analysis, and so the cubic phonons are retained as reference modes for consistency with other sections of this work. The coefficients of the six important modes are thus taken as order parameters. However, they may be grouped into two sets according to the points of the cubic Brillouin Zone at which they are found, and whether they are invoked in forming the tetragonal or orthorhombic phase.

In principle, the Fourier transform of each coefficient $c_j(t)$ should generate a partial density of states (DOS) $\tilde{c}_j(\nu)$, which for a perfectly harmonic mode would show a single frequency. However, a MD simulation of time τ will give a frequency resolution of $1/\tau$, typically 1 THz in these simulations. Furthermore, few of the phonons are perfectly harmonic, and phase transformations during the simulation introduce other Fourier components and frequency shifts. The longest simulation was done at a temperature of around 850 K, and the two phonons found to give the clearest partial DOS are shown in Fig. 3 by way of example. These modes are thus the least affected by the transition to the orthorhombic phase which takes place during the simulation. Both modes involve Mg displacements along z, so would be expected to be only weakly coupled to those involved in the transition which are in the xy plane. Longer simulations would, however, be required for definitive results from such a process.

Low temperature

At temperatures below T_c, the orthorhombic phase is expected to be stable; this requires freezing in the four modes listed above. From an assigned temperature of 800 K the system first appeared to equilibrate around 430 ± 5 K (as might be expected by equipartition), but after 300 fs the temperature increased to 550 ± 5 K. This was accompanied by a distinct increase in the total distortion $\langle |\mathbf{d}|^2 \rangle_t$ from 40.82 ± 0.09 to 52.0 ± 0.5 a.m.u. Å^2, as shown in Fig. 4.

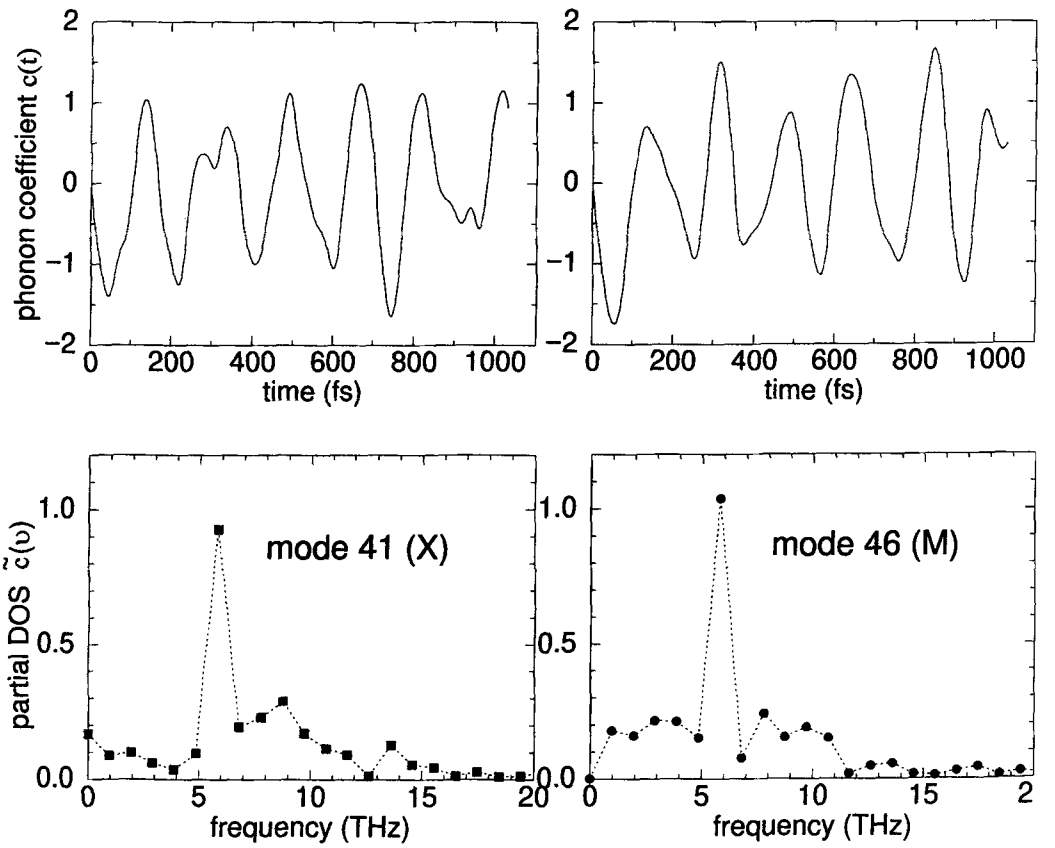

FIG. 3. Phonon coefficients $c_j(t)$ and partial density of states (Fourier transform) $\tilde{c}_j(\nu)$ for two modes which give the clearest single frequencies in a MD simulation around 850 K. Both modes involve Mg displacement along the z axis. The plotted points demonstrate the maximum resolution available from a 1 ps simulation.

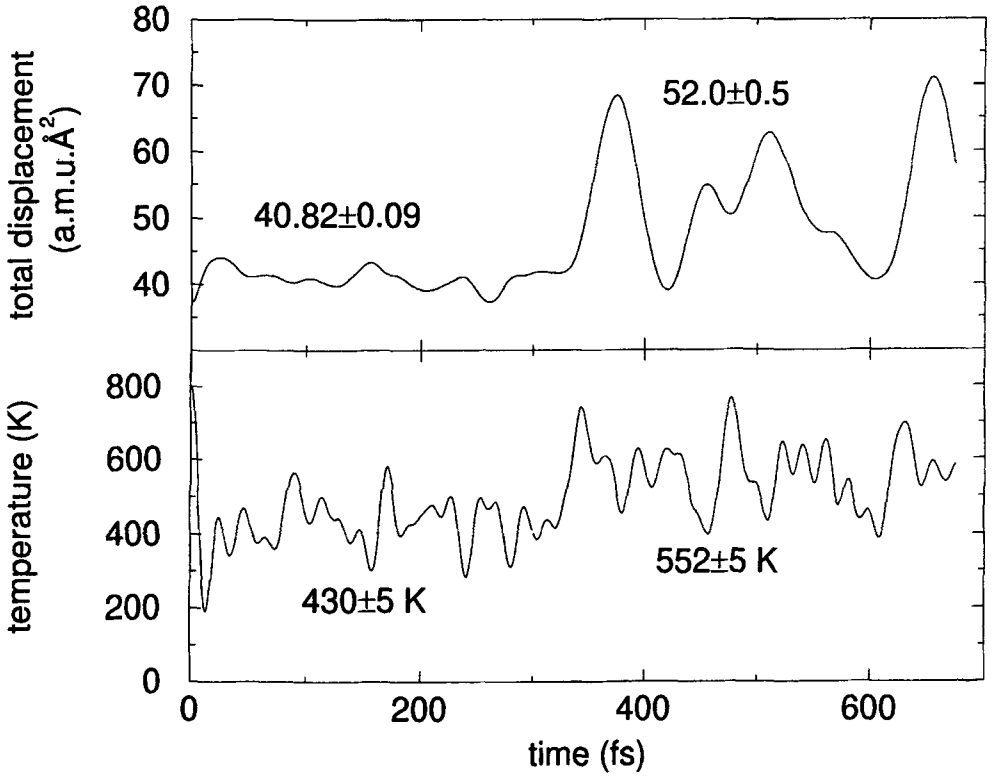

FIG. 4. Total distortion from cubic $|\mathbf{d}(t)|^2$ (upper graph) and temperature as found from kinetic energy (lower) during a simulation at low temperature.

The coefficients of selected phonons during this simulation are shown in Fig. 5. The R modes which form the tetragonal phase, §59/60 and §47/48, have significant coefficients throughout, as would be expected. During the first half of the simulation, the third R_{25} rotational phonon §58, which is still unstable in the tetragonal phase, acquires a large amplitude, whilst the M_2 mode §57 is present only weakly. However, after 300 fs the M_2 mode acquires a large average coefficient, and oscillates around that value without crossing $c(t) = 0$, whilst mode §58 returns to small oscillations about zero. Accompanying this change are increases in the coefficients of §13, §30/31 and §50/51, i.e. those known to be present in the orthorhombic phase. The system is thus identified as orthorhombic in this part of the simulation. The transition into the orthorhombic phase is also manifested by an increase in the total distortion and explains the increase in temperature at this point. The observation that the four modes contributing to the orthorhombic phase freeze into the structure simultaneously is further confirmation that these modes are strongly coupled together, and that there it is unlikely that there are further intermediate phases between the tetragonal and orthorhombic phases with compatible symmetry.

The M_2 phonon §57 as shown here has a frequency of approximately 6.9 THz. This is about half of the frequency calculated in the orthorhombic phase; the difference may be ascribed to anharmonicity and coupling, since the oscillations are by no means small. Although different pseudopotentials were also used in the initial calculations, the changes in frequency of the rotational phonons in the cubic phases were relatively small (Warren and Ackland, 1996).

Intermediate temperatures

A simulation at an intermediate temperature appeared to equilibrate around 850 K after about 300 fs, after an inital average displacement $\langle|\mathbf{d}|^2\rangle_t$

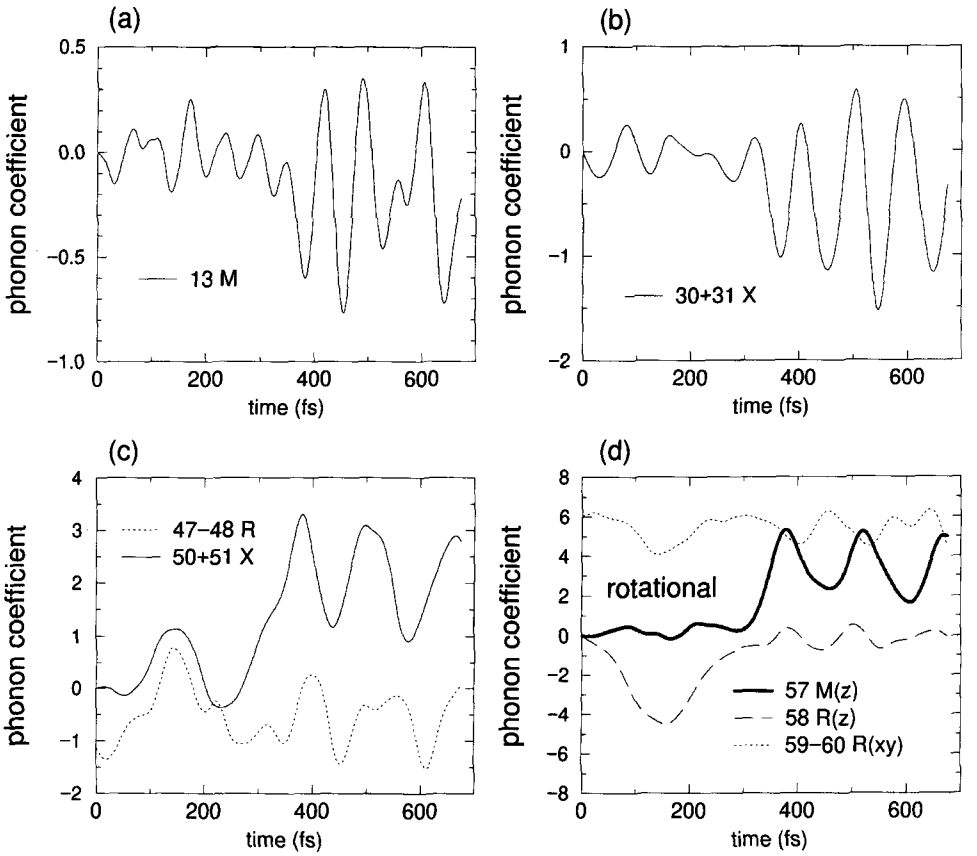

FIG. 5. Phonon coefficients (in a.m.u. Å^2) for all modes with significant $\langle c(t)\rangle_t$ during the low-temperature MD simulation. The modes in (d) primarily involve rotations of the SiO_6 octahedra.

of 43.6 ± 0.1 a.m.u. Å^2 increased to 52.7 ± 0.3 a.m.u. Å^2. The dominant phonons are shown in Fig. 6. It can be seen that the M_2 mode §57 freezes in but almost immediately changes sign, as does §50/51 and to a less dramatic extent, §30/31 and §13. The coupling between these four modes is again evident from the simultaneous switching of sign. This jump from one of the orthorhombic phases to an equivalent demonstrates the increasing thermal energy invested in these modes. In contrast, the modes at R which constitute the tetragonal phase, §47/48, §58 and §59/60, are mostly unaffected by these changes.

High temperature

At 1750 K, a significant contribution from §57 and related modes is seen (Fig. 7), indicating that the system is still orthorhombic. A distinct increase in total displacement was again observed, from $\langle |\mathbf{d}|^2 \rangle_t = 48.7 \pm 0.3$ to 56.9 ± 0.4 a.m.u. Å^2.

However, the metastable tetragonal phase is observed for the first 650 ps of the simulation, and includes significant contributions from mode §58. This is not surprising, since modes §58, §59 and §60 are triply degenerate in the cubic phase, and §58 is almost as unstable as §57 in the tetragonal. It can be seen that the coefficient of §58 increases at the expense of §59/60, so only one mode constitutes the tetragonal phase. The structure formed by freezing in all three of these modes also has lower symmetry than the tetragonal, so would be considered as an alternative to the orthorhombic phase, rather than as a possible intermediate towards the cubic.

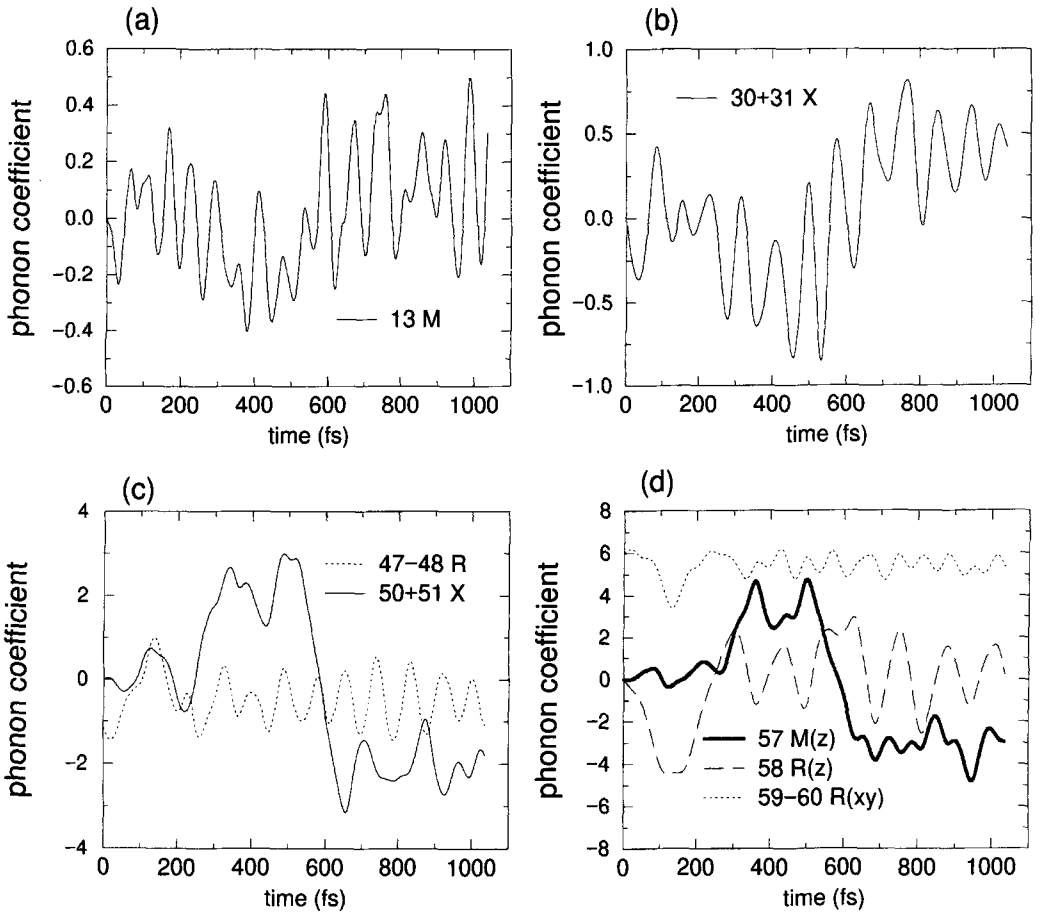

FIG. 6. Phonon coefficients (in a.m.u. Å^2) for all modes with significant average amplitude during the intermediate MD simulation. The modes in (d) primarily involve rotations of the SiO_6 octahedra.

Implications for T_c

It appears that at zero pressure an orthorhombic–tetragonal transition would require a higher temperature than 1750 K, and thus higher than the melting temperature. If coupling to the strain is allowed, the energy difference between these phases increases (Warren and Ackland, 1996), thus further increasing T_c. At higher pressures, such as those found in the mantle, the denser orthorhombic phase would be increasingly favoured, although the melting temperature also increases. These MD studies thus suggest that the transition does not occur in the mantle.

However, these simulations are not only limited by neglecting coupling to the strain, but also by the simulation of only twenty atoms. Phase transitions usually involve long-range fluctuations close to the transition temperature, which are explicitly excluded by periodic boundary conditions. Furthermore, the finite duration of these simulations, necessary because of the extreme levels of computational resources required, means that the long-term behaviour may not be adequately represented. More extensive simulations would therefore improve the reliability of these predictions. Simulations away from T_c could also be used to deduce T_c by extrapolation of quantities such as the change in free energy, but good statistics would again be needed.

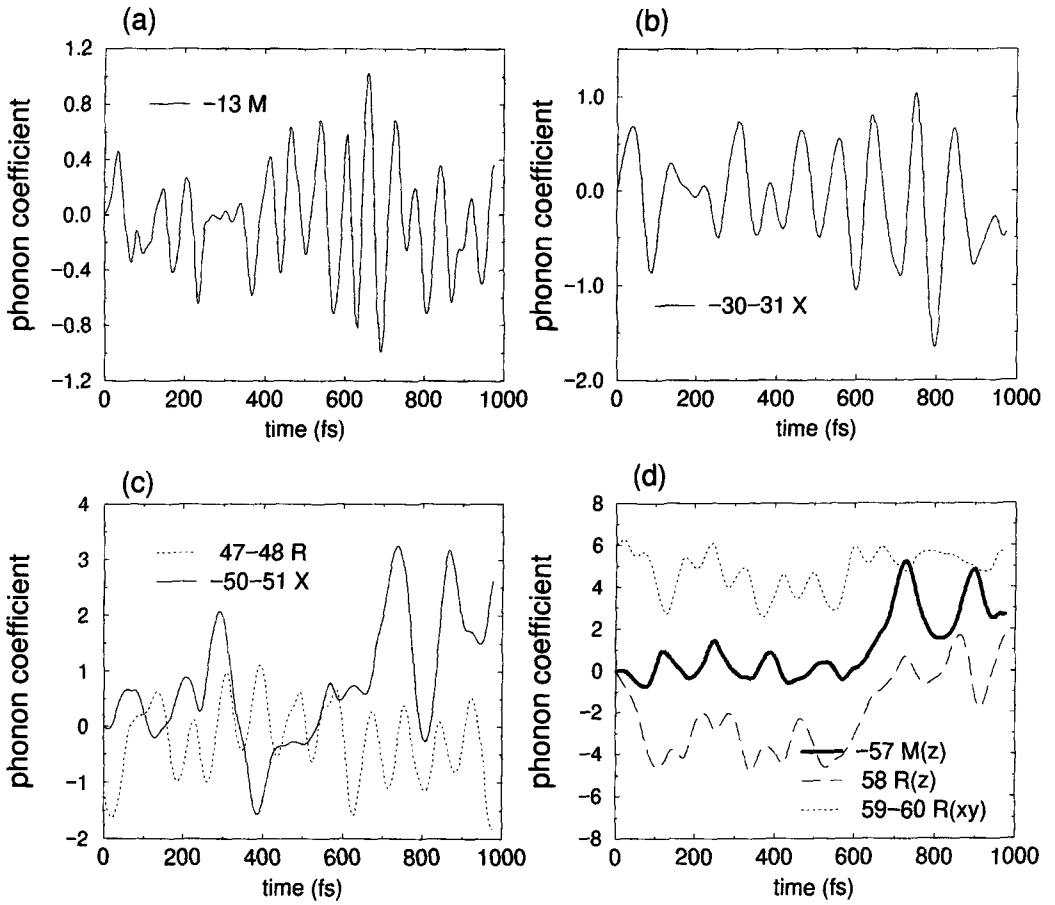

FIG. 7. Phonon coefficients (in a.m.u. Å^2) for all significant modes during the high temperature simulation. The modes in (d) primarily involve rotations of the SiO_6 octahedra.

Calcium silicate

Recent first-principles studies (Stixrude *et al.*, 1996) using the Linear Augmented Plane Wave (LAPW) method have found that cubic $CaSiO_3$ perovskite also has an instability with respect to tilting of the octahedra, primarily at the *R* point of the Brillouin Zone. $CaSiO_3$ is conventionally taken to be stable in the cubic phase, since no deviation from the cubic structure has been observed experimentally (Wang *et al.*, 1996). In contrast, this instability would imply that the stable state in fact has lower symmetry. LAPW simulations consider all electrons, not just the valence electron states which are found with pseudopotentials. However, full structural optimisations using pseudopotentials have found the cubic phase to be stable (Wentzcovitch *et al.*, 1995). Both these sets of calculations used the local density approximation (LDA).

We calculated the phonons at Γ, *X*, *M* or *R* at zero pressure and at 80 GPa, using the CASTEP code with the LDA and a basis set converged to better than 0.002 eV/unit. No unstable modes were found at either pressure, and a trend of increasing frequencies with pressure. The R_{25} rotation modes did, however, have very low frequencies (2.0 THz at 0 GPa, rising to 4.5 THz at 80 GPa). Furthermore, full structural relaxation of a tetragonal phase with an R_{25} octahedral rotation reverted to the cubic undistorted phase. An orthorhombic (*Pbnm*) phase

analogous to that in $MgSiO_3$ also returned to cubic symmetry on relaxation. Our calculations are thus in agreement with the previous pseudopotential calculations (Wentzcovitch *et al.*, 1995), which are used as a different approach in order to determine the stability, and suggest that the cubic phase is stable.

Such instabilities are usually very strongly coupled to the cell volume, so further calculations currently in progress aim to clarify the effect of pressure.

The instability predicted by the LAPW calculations would produce a tetragonal phase with energy only 0.12 eV per unit cell lower than the cubic phase. This energy difference is large enough to be found with pseudopotential plane-wave calculations, but only when great care is taken to fully converge the calculation with respect to k-point sampling of the electronic bandstructure and number of plane waves. It may be that such weak instabilities are particularly sensitive to differences in theoretical techniques.

Conclusions

The structures and important sets of phonons of cubic, tetragonal and orthorhombic phases of $MgSiO_3$ have been found from first principles. The unstable phonons of the cubic structure are distributed throughout the Brillouin Zone, but all become stable after the transition to the orthorhombic structure. No such instabilities are found in $CaSiO_3$ perovskite.

By freezing in the most unstable phonon of the cubic phase, and another strongly coupled to it, a tetragonal intermediate may be formed, which displays some of the structural features of the orthorhombic phase. The eigenvectors of the most unstable phonon of this phase, and those coupled to it, contain the remaining distortions necessary to reach the orthorhombic phase. Rotations of octahedra play the largest part in the transition.

A two stage transition pathway between the cubic and orthorhombic phases may be expressed in terms of only six phonons, and small strains of the unit cell. Molecular dynamics simulations of one of these stages are analysed in terms of these phonons, with the result that a transformation from a metastable tetragonal phase to the orthorhombic is clearly identifiable. However, the transition was always observed for temperatures up to 1750 K, which is close to the melting temperature. These results suggest that the transition temperature for the tetragonal–orthorhombic transition is thus likely to be too high for the tetragonal phase to occur in the mantle. Further study would be necessary on larger systems for longer times to confirm this prediction; allowing the unit cell to change size and shape during the simulations would also be necessary for more realistic simulations.

Acknowledgements

The authors thank the Edinburgh Parallel Computing Centre for use of the Cray T3D. S.J.C. and M.C.W. thank the E.P.S.R.C. and B.B.K. the University of Edinburgh for support, and M.C.W. thanks Keith Refson for valuable comments.

References

Ackland, G., Warren, M. and Clark, S. (1997) Practical methods in ab initio lattice dynamics, *J. Phys.: Cond. Mat.*, **9**, 7861–72.

Bukowinski, M. and Wolf, G. (1988) Equation of state and possible critical phase transitions in $MgSiO_3$ perovskite at lower-mantle conditions. In: *Structural and Magnetic Phase Transitions in Minerals*, (S. Ghose, J. Coey and E. Salje, eds.). Springer-Verlag, New York, pp. 91–112.

Car, R. and Parrinello, M. (1985) Unified approach for molecular dynamics and density-functional theory. *Phys. Rev. Lett.*, **55**, 2471–4.

Catlow, C. and Price, G. (1990) Computer modelling of solid-state inorgaic materials. *Nature*, **347**, 243–8.

Clark, S. and Ackland, G. (1997) Ab initio calculations of the self-interstitial in silicon. *Phys. Rev.*, **B56**, 47–50.

Clarke, L., Stich, I. and Payne, M. (1992) Large-scale ab initio total energy calculations on parallel computers. *Comp. Phys. Comms.*, **72**, 14–28.

Cohen, R. and Krakauer, H. (1990) Lattice dynamics and origin of ferroelectricity in $BaTiO_3$: Linearized-augmented-plane-wave total-energy calculations. *Phys. Rev.*, **B42**, 6416–23.

Francis, G. and Payne, M. (1990) Finite basis set corrections to total energy pseudopotential calculations. *J. Phys.: Cond. Mat.*, **2**, 4395–404.

Giddy, A., Dove, M., Pawley, G. and Heine, V. (1993) The determination of rigid-unit modes as potential soft modes for displacive phase transitions in framework crystal structures. *Acta. Cryst.*, **A49**, 697–703.

Hemley, R. and Cohen, R. (1992) Silicate perovskite. *Ann. Rev. Earth Planet. Sci.*, **20**, 553–600.

Hemley, R., Jackson, M. and Gordon, R. (1987) Theoretical study of the structure, lattice dynamics,

and equations of state of perovskite-type $MgSiO_3$ and $CaSiO_3$. *Phys. Chem. Minerals*, **14**, 2–12.

Hsueh, H., Warren, M., Vass, H., Ackland, G., Clark, S. and Crain, J. (1996) Vibrational properties of the layered semiconductor germanium sulfide under hydrostatic pressure. *Phys. Rev.*, **B53**, 14806–17.

Karki, B., Stixrude, L., Clark, S., Warren, M., Ackland, G. and Crain, J. (1997) Elastic properties of orthorhombic $MgSiO_3$ perovskite at lower mantle pressures. *Amer. Mineral.*, **82**, 635–8.

Kerker, G. (1980) Non-singular atomic pseudopotentials for solid-state applications. *J. Phys.*, **C13**, L189–94.

King-Smith, R. and Vanderbilt, D. (1994) First-principles investigation of ferroelectricity in perovskite compounds. *Phys. Rev.*, **B49**, 5828–44.

Kleinman, L. and Bylander, D. (1982) Efficacious form for model pseudopotentials. *Phys. Rev. Lett.*, **48**, 1425–8.

Lines, M. and Glass, A. (1977) *Principles and Applications of Ferroelectrics and Related Materials*, Clarendon Press, Oxford.

Mao, H., Hemley, R., Fei, Y., Shu, J., Chen, L., Jephcoat, A., Wu, Y. and Bassett, W. (1991) Effect of pressure, temperature and composition on lattice parameter and density of $(Fe,Mg)SiO_3$–perovskites to 30 GPa. *J. Geophys. Res.*, **96**, 8069–79.

Matsui, M. (1988) Molecular dynamics study of $MgSiO_3$ perovskite. *Phys. Chem. Miner.*, **16**, 234–8.

Navrotsky, A. and Weidner, D. (eds) (1989) *Perovskite: A Structure of Great Interest to Geophysics and Materials Science*. American Geophysical Union.

Oguchi, T. and Sasaki, T. (1991) Density-functional molecular-dynamics method. *Prog. Theor. Phys.*, Supp. **103**, 93–117.

Payne, M., Teter, M., Allan, D., Arias, T. and Joannopoulos, J. (1992) Iterative minimisation techniques for ab initio total-energy calculations: molecular dynamics and conjugate gradients. *Rev. Mod. Phys.*, **64**, 1045–97.

Postnikov, A., Neumann, T. and Borstel, G. (1994) Phonon properties of $KNbO_3$ and $KTaO_3$ from first-principles calculations. *Phys. Rev.*, **B50**, 758–63.

Rabe, K. and Waghmare, U. (1996) Ferroelectric phastransitions from first principles. *J. Phys. Chem. Solids*, **57**, 1397–403.

Ross, N. and Hazen, R. (1990) High-pressure crystal chemistry of $MgSiO_3$ perovskite. *Phys. Chem. Miner.*, **17**, 228–37.

Stixrude, L. and Cohen, R. (1993) Stability of orthorhombic $MgSiO_3$ perovskite in the earth's lower mantle. *Nature*, **364**, 613–6.

Stixrude, L., Cohen, R., Yu, R. and Krakauer, H. (1996) Prediction of phase transition in $CaSiO_3$ perovskite and implications for lower mantle structure. *Amer. Mineral.*, **81**, 1293–6.

Wang, Y., Guyot, F. and Liebermann, R. (1992) Electron microscopy of $(Mg,Fe)SiO_3$ perovskite: evidence for structural phase transitions and implications for the lower mantle. *J. Geophys. Res.*, **97**, 12327–47.

Wang, Y., Weidner, D. and Guyot, F. (1996) Thermal equation of state of $CaSiO_3$ perovskite. *J. Geophys. Res.*, **101**, 661–72.

Warren, M. and Ackland, G. (1996) Ab initio studies of structural instabilities in magnesium silicate perovskite. *Phys. Chem. Miner.*, **23**, 107–18.

Wentzcovitch, R., Martins, J. and Price, G. (1993) Ab initio molecular dynamics with variable cell shape: Application to $MgSiO_3$. *Phys. Rev. Lett.*, **70**, 3947–50.

Wentzcovitch, R., Ross, N. and Price, G. (1995) Ab-initio study of $MgSiO_3$ and $CaSiO_3$ perovskites at lower-mantle pressures. *Phys. Earth. Planet. Int.*, **90**, 101–12.

[*Revised manuscript received 2 May 1998*]